Multi-view Laplacian Least Squares For Human Emotion Recognition

Shuai Guo[a], Lin Feng[a,*], Zhan-Bo Feng[b], Yi-Hao Li[b], Yang Wang[a], Sheng-Lan Liu[a], Hong Qiao[c]

[a]*School of Innovation and Entrepreneurship, Dalian University of Technology, Dalian 116024, China*
[b]*School of Electronic Information and Electrical Engineering, Dalian University of Technology, Dalian 116024, China*
[c]*State Key Laboratory of Management and Control for Complex Systems, Institute of Automation, Chinese Academy of Sciences, Beijing 100190, China*

Abstract

Human emotion recognition is an emerging and important area in the field of human-computer interaction and artificial intelligence, which has been more and more related with multi-view learning methods. Subspace learning is an important direction of multi-view learning. However, most existing subspace learning methods could not make full use of both category discriminant information and local neighborhood information. As a typical subspace learning method, partial least squares (PLS) performs better and more robustly than many other subspace learning methods, because PLS is optimized with iteration method. However, PLS suffers from linear relationship assumption and two-view limitation. In this paper, a new nonlinear multi-view laplacian least squares (MvLLS) is proposed. MvLLS constructs a global laplacian weighted graph (GLWP) to introduce category discriminant information as well as protects the local neighborhood information. Optimized with iteration method, MvLLS is a multi-view extension of PLS. The proposed method has great extendibility and robustness. To meet the requirements of large-scale applications, weighted local preserving embedding (WLPE) is proposed as the out-of-sample extension of MvLLS, basing on the idea of maintaining the manifold structures of original space. Finally,

*Corresponding author
Email address: fenglin@dlut.edu.cn (Lin Feng)

the proposed method is verified on three multi-view emotion recognition tasks, the experiment results validate the effectiveness and robustness of MvLLS.
Keywords: Multi-view learning, Laplacian Least Squares, Subspace learning, Human emotion recognition
2010 MSC: 00-01, 99-00

1. Introduction

Human emotion recognition is a long-standing and emerging problem in computer vision and human-computer interaction, where there have been many significant researches. Most early human emotion recognition researches focused on single view learning methods, such as image-based face emotion recognition [1], video-based body emotion recognition [2, 3], speech emotion recognition [4], and physiological signal emotion recognition [5, 6, 7]. However, human emotion can be observed at various viewpoints, even by different sensors. Recently, many multi-view human emotion recognition methods [8, 9, 10] were proposed to learn feature from each view effectively and improve the recognition accuracy. One effective approach of multi-view learning is subspace learning [11, 12], which aims at getting a common subspace shared by various views. Compared with other approaches, subspace learning considers similarities and differences of all views to get a low-dimensional embedding for each view, Subspace learning is effective in reducing curse of dimensionality, and has been widely used in many aspects of machine learning.

Although many significant subspace learning methods have been proposed, there is still much room for improvement. The motivations of this paper are twofold:

(1) There are few methods could balance the scatter discriminant information and protect the local neighborhood information in the mean time. Existing subspace learning methods mainly focus on cross correlation, scatter discriminant information or local neighborhood information.

(2) PLS get much better performance in practical applications compared with canonical correlation analysis (CCA) [13], even they have similar optimization targets. However, traditional PLS suffers from the basic assumption that latent linear relationships exist between different views, and the basic framework of PLS is difficult to extend to more views.

In this paper, we present a nonlinear multi-view laplacian least squares (MvLLS) method for the human emotion recognition. The contributions and characters of our work are threefold.

(1) Inspired by laplacian eigenmaps (LE) [14], a global laplacian weighted graph (GLWP) is constructed across all views, where the local neighbor information is maintained and category discriminant information is introduced.

(2) Traditional PLS is upgraded to a supervised, nonlinear and multi-view modification MvLLS.

(3) To accommodate the large-scale applications, an out-of-sample method weighted local preserving embedding (WLPE) is presented to process new samples.

The remainder of this paper is organized as follows. Section 2 defines the common notations and review some preliminary works. Then Section 3 introduces the formulations and optimizations of MvLLS in detail, as well as some extensions. After that, Section 4 presents the experimental results and quantitative evaluations, followed by a conclusion.

2. Preliminary works

In this section, existing works on multi-view subspace learning are introduced as a whole in Section 2.1. Then common notations used throughout this paper are defined in Section 2.2. After that, some researches that are related to our work are introduced in Section 2.3, including PCA, CCA, LE, PLS and MvDA.

2.1. Summary

Generally speaking, existing subspace learning based multiview learning methods can be divided into three categories according to their key ideas:

Maximize the cross correlations. This line of methods mainly come from canonical correlation analysis (CCA) [13], which attempts to learn two linear transforms for each view to maximize their cross correlation in the subspace. Kernel CCA (KCCA) [15], multiview CCA (MCCA) [16] are the kernel and multiview extensions of CCA respectively. Partial least squares (PLS) [17] uses iterative method and least square regression to approximate an optimization problem that is similar to CCA, but with different constraints. The kernel version of PLS was introduced in [18]. And a single optimization termed method SVM-2K that combines SVM and KCCA was proposed in [19]. Multi-view SVM-2K [20] presents a multi-view modification for SVM-2K. In addition, a nonparametric sparse matrix and automatic model were proposed for multi-feature fusion in [21], by imposing label information across all views to exploit the correlations. Recently, a hierarchical multi-view multi-feature fusion method (HMMF) [22] was proposed by using a sparse covariance matrix to represent the correlations over all views. However, HMMF has a great spatiotemporal complexity.

Balance the scatter discriminant information. Inspired by linear discriminant analysis (LDA) [23], the scatter discriminant information of multi-view learning refers chiefly to within-class, between-class, intra-view or inter-view discriminants. Protecting the discriminant structure contributes to get samples of the same class together and separate samples of different classes. Correlation discriminant analysis (CDA) [24] is a supervised improvement of CCA basing on the definitions of within-class correlation and between-class correlation. A generalized multi-view analysis framework (GMA) which considers the intra-view discriminant information in the common subspace was proposed in [25]. Multi-view discriminant analysis (MvDA) [26] gets a linear transform for each view by maximizing the between-class variations and minimizing the within-class variations across all views. And MvDA-VC [26] was proposed basing on MvDA by adding view-consistency. Besides, multi-view uncorrelated discriminant analysis (MULDA) [27] combines uncorrelated LDA [28] with CCA to preserve both category discriminant information and correlation information. A generalized

multi-view embedding method (GME) [29] was proposed for CCA, PLS and LDA, using intrinsic and penalty graphs to characterize the intra-view and inter-view discriminant information. And laplacian multi-set canonical correlations (LaMCCs) [30] constructs the nearest neighbor graphs to take intra-view and inter-view correlations into consideration. Multi-view local discrimination and canonical correlation analysis (MLDC^{2}A) [31] aims at optimizing a combination of between-class scatter, within-class scatter and correlation. And in [32], a novel end-to-end place recognition model was proposed, which encode the spatial and structural information to let feature representations process more discriminant power.

Protect the local neighborhood information. Protecting the local characteristics would help in maintaining the manifold structures. Multi-view spectral embedding (MSE) was developed to obtain a smooth low-dimensional embedding across multiple views in [33]. And locality-preserving CCA (LPCCA) [34] integrates the local neighborhood information together with CCA to discover the low-dimensional manifold structures for different views. To solve the problem of large pose variations and facial expression recognition, locality-constrained linear coding was utilized to construct the model in [35]. A graph regularized multi-set canonical correlations (GrMCC) [36] was proposed to utilize discriminative and intrinsic geometrical information under the framework of correlation analysis. Recently, noticing that Hessian can exploit the intrinsic local geometry of data, Hessian multiset CCA [37] showed superior extrapolating capability with nonlinear multi-view features. In [38], a novel pose recovery frame was proposed by simultaneously learning the task of joint localization and detection.

Note that some of these methods may have more than two of the three ideas mentioned above, they are still classified with the most important idea. Besides, there are many significant single view subspace learning methods or dimensional reduction methods based on graph learning. Locality constrained graph optimization dimensionality reduction (LC-GODR) [39] that combines the graph optimization and projection matrix learning can be adaptively updated. In [40], a multi-kernel locality-constrained collaborative representation-based classifier

(MKLCRC) utilized local structures to improve classification performance. And a multiview locality-sensitive sparse retrieval was proposed in [41] to perform the 3-D human pose recovery, by incorporating a local similarity and integrating multiview data.

2.2. Notations

Given samples of various different views and their labels, subspace learning methods expect to learn a low-dimensional embedding in the common subspace for each view. Important notations in this paper are listed in Table 1:

Table 1: Definitions of important notations

Notation	Description
$X_i \in \mathbb{R}^{d_i \times n_i}$	All n_i samples of i^{th} view
$Label_i \in \mathbb{R}^{n_i}$	Labels that correspond to samples in X^i
$x_{ia}, x_{jb} \in \mathbb{R}^d$	The a^{th} and b^{th} of view X_i and X_j
$label_{ia}, label_{jb}$	The labels of x_{ia} and x_{jb}
v	The number of views
c	The number of class across all views
dim	Dimension of the subspace
$w_i \in \mathbb{R}^{d_i}$	The linear transform of X_i
$Y_i \in \mathbb{R}^{dim \times n_i}$	The embedding of X_i in the subspace
$y_{ia}, y_{jb} \in \mathbb{R}^{dim}$	The embeddings of x_{ia} and x_{jb}
$y^i \in \mathbb{R}^{n_i}$ $y^j \in \mathbb{R}^{n_j}$	One dimensional features of samples of X_i and X_j in the subspace
W_{ab}^{ij}	The weight of connection between x_{ia} and x_{jb}
I	The identity matrix
$tr(X)$	Trace of matrix X

When we refer to single-view learning methods, the view $X \in \mathbb{R}^{d \times n}$ is used. And when we refer to methods that require the equality of number of samples, n

is used instead of n_i. In some other specific situations, we would remove upper and lower corner markers as needed.

2.3. Related methods

2.3.1. PCA and CCA

PCA [42] is a classical dimensional reduction (DR) and single view learning method. With normalization as the first step, PCA finds a group of standard orthogonal basis to maximum the variance of view X after projection, which can be transformed as the trace of covariance matrix of projection of X:

$$\begin{aligned} &\max_{w} w^T X X^T w \\ &s.t.\ w^T X X^T w = 1 \end{aligned} \tag{1}$$

CCA [13] is a two-view learning method that attempts to find two linear transforms w_1 and w_2 for the normalized feature matrices X_1 and X_2, such that their embeddings in the common subspace are most correlated:

$$\begin{aligned} &\max_{w_1, w_2} w_1^T X_1 X_2^T w_2 \\ &s.t.\ w_1^T X_1 X_1^T w_1 = 1, w_2^T X_2 X_2^T w_2 = 1 \end{aligned} \tag{2}$$

Eq. (1) and Eq. (2) can be solved by using Lagrange multiplier method. CCA can be regarded as the two-view version of PCA. And one of the main drawbacks of CCA is that the number of samples of the two views must be equal.

2.3.2. Laplacian eigenmaps

Laplacian Eigenmaps (LE) [14] is an effective single-view nonlinear manifold learning method. Given the n samples of X, LE has great locality preserving properties by constructing a weighted graph W:

$$W_{ab} = \begin{cases} exp(-\frac{\|x_a - x_b\|_2^2}{t}), & if\ \|x_a - x_b\|_2^2 < \epsilon \\ 0, & else \end{cases} \tag{3}$$

In W, the neighboring samples are connected with weighted edges to record the locality information. Let y_a and y_b denote the low-dimensional representation of a^{th} and b^{th} sample, LE maps the weighted graph W to a low-dimensional space with connected samples stay as close together as possible:

$$\begin{aligned} \min_{Y} \frac{1}{2} \sum_{a,b} \|y_a - y_b\|_2^2 W_{ab} &= \min_{Y} tr(Y^T L Y) \\ s.t.\ Y^T D Y &= I \\ D_{kk} = \sum_{j=1}^{n} W_{jk},\ L &= D - W \end{aligned} \tag{4}$$

In Eq. (4), D is a diagonal matrix and L is the laplacian matrix. This equation can be solved by computing eigenvalues and eigenvectors of a generalized eigenvector problem.

2.3.3. Partial least squares

Partial least squares regression (PLS) [17] has similar optimization target to CCA, it can be regarded as a linear unsupervised two-view learning method. Traditional PLS maximizes the correlation of the two views after projection. PLS supposes that the two views can be driven by a few latent variables, which are not directly observed or measured. PLS uses iterative method to predict X_2 with X_1 by finding the component of X_1 and using it as the regressor of both views. After each iteration step, X_1 and X_2 are covered by the residual matrices E and F:

$$\begin{aligned} \max_{w_1,w_2} y_1 y_2^T &= \max_{w_1,w_2} w_1^T X_1 X_2^T w_2 \\ s.t.\ w_1^T w_1 = 1, w_2^T w_2 &= 1 \\ X_1 = P^T Y_1 + E \\ X_2 = Q^T Y_2 + F \\ Y_2 = D Y_1 + H \end{aligned} \tag{5}$$

PLS supposes X_1 and X_2 have the same number of samples like CCA, that is $n_1 = n_2 = n$. In Eq. (5), $P \in \mathbb{R}^{dim \times d_1}$, $Q \in \mathbb{R}^{dim \times d_2}$ are the loading matrices. $E \in \mathbb{R}^{d_1 \times n}$, $F \in \mathbb{R}^{d_2 \times n}$ and $H \in \mathbb{R}^{dim \times n}$ are the residual matrices. And $D \in \mathbb{R}^{dim \times dim}$ shows the latent scores of two views. But in multi-view learning, the latent linear relationship between different views do not always exist.

2.3.4. Multi-view discriminant analysis

Inspired by LDA [23], the main idea of MvDA [26] is to find v linear transforms to project samples of all views to a common subspace, where the between-class variation S_B^y is maximized and the within-class variation S_W^y is minimized.

$$\begin{aligned} &\max_{w_1,\cdots,w_v} \frac{tr(S_B^y)}{tr(S_W^y)} \\ S_W^y &= \sum_{i=1}^{v}\sum_{j=1}^{c}\sum_{k=1}^{n_{ij}}(y_{ijk}-\mu_j)(y_{ijk}-\mu_j)^T \\ S_B^y &= \sum_{i=1}^{c} n_i(\mu_i-\mu)(\mu_i-\mu)^T \end{aligned} \tag{6}$$

In Eq. (6), n_{ij} is the number of samples that are labeled as j in X_i, y_{ijk} is the label of k^{th} sample in X_i that is labeled as j, μ_j is the mean of low-dimensional embeddings of all samples in the v views that are labeled as j, and μ is the mean of low-dimensional embeddings of all samples in the v views. Supposing that each view can be a flipping of any other one, MvDA-VC is proposed by adding a view-consistency term to the denominator of Eq. (6).

MvDA and MvDA-VC take both between-class and within-class discriminant information into consideration. They can deal with the cases where there are different number of samples or classes for the v views. However, the integrity and local structure of a single view is broke up, as S_W^y and S_B^y are calculated across all views.

3. Multi-view laplacian least squares

3.1. Overview

In this section we present the detailed ideas and optimizations of multi-view laplacian least squares (MvLLS), followed with some extensions. Basing on the frameworks of LE and PLS, MvLLS is proposed to get the nonlinear subspace embedding of each view directly. MvLLS aims to find a subspace for all views where the connected samples stay as close together as possible. In Section 3.2, the global laplacian weighted graph (GLWP) $\mathcal{W}$ is constructed over all views. GLWP can not only protect the local geometry structure, but also introduce the category discriminant information. As features of the v views lie on different dimensions, a DR framework should be applied to make samples of different views measurable. The basic idea and usage of DR framework are shown in Fig. 1. In Section 3.3, inspired by PLS, laplacian partial least squares (LPLS) is used to solve the optimization problem. We remove the estimated variations and update $\mathcal{W}$ in each iteration, the variations are predicted by low-dimensional embeddings of views. In Section 3.4, to accommodate the large-scale applications, an out-of-sample extension method weighted local preserving embedding (WLPE) is introduced to get the embeddings of new samples. WLPE attempts to maintain the high-dimensional local neighborhood information in the subspace. In Section 3.5, some extensions of MvLLS are presented.

The proposed method takes both advantages of scatter discriminant balance and locality protection. With a robust weighted graph, MvLLS can deal with the lack of partial samples or category information. One of the great advantages over other methods is that, MvLLS can also work on unsupervised or semi-supervised models, even cases that the number of samples are different for the given views. Moreover, as the weighted graph varies by iteration, the change rate can be used to predict the intrinsic dimension of the subspace got by MvLLS.

3.2. Global laplacian weighted graph

In this section we construct the global laplacian weighted graph that weights the connections of samples across all views, and get the embeddings of all sam-

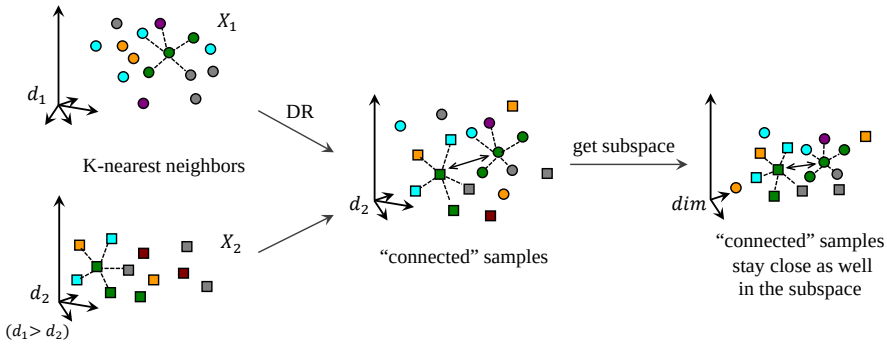

Fig. 1: The basic idea of MvLLS, with X_1 and X_2 as an example. Squares and circulars denote samples from X_1 and X_2 respectively, labels of samples are represented by different colors. a DR frameworks is used to get a common space for X_1 and X_2. Whether samples are connected or not depends on labels of themselves and their neighbors. And the connected samples would stay close as well in the subspace got by MvLLS.

ples on one dimension of the subspace, which are $y^1, \cdots, y^v$. MvLLS tries to find a subspace in which the connected samples of each pair views stay as close together as possible.

We talk about connections between two views firstly, with X_i and X_j as an example:

$$\begin{aligned}\min_{y^i, y^j} \xi(i,j) &= \frac{1}{2} \sum_{\substack{1 \le a \le n_i \\ 1 \le b \le n_j}} \|y_{ia} - y_{jb}\|_2^2 W_{ab}^{ij} \\ &= \frac{1}{2} \sum_{a,b} (y_{ia}^2 + y_{ib}^2 - 2 y_{ia} y_{ib}) W_{ab}^{ij} \\ &= y^i L^{ij} y^{jT} \\ D_{kk} = \sum_{j=1}^{n_i} W_{jk},\ & L^{ij} = D - W^{ij}\end{aligned} \tag{7}$$

In Eq. (7), y^i denotes one dimensional features of samples of X_i in the subspace, each element of y^i represents the one dimensional feature of a sample. $W^{ij} \in \mathbb{R}^{n_i \times n_j}$ is a weighted matrix which measures the weights of connections between samples of X_i and X_j, D is a diagonal matrix, and L^{ij} is the laplacian

matrix corresponds to W^{ij}. When i is not equal to j, connections between samples of different views are considered. And when i is equal to j, connections between samples of the same view are considered. As the dimensions of the two views are different, a DR framework is used to project X_i and X_j to a common dimension which is the minimum of d_i and d_j. Any proper algorithms could be used to realized DR framework, according to different demands. The algorithm we used in the experiments behind is principal component analysis (PCA) [42], as it is classical, effective and widely used. And in W^{ij}, the weighted edge W^{ij}_{ab} that connects X_{ia} and X_{jb} is defined as below:

$$W^{ij}_{ab} = \begin{cases} exp(-\frac{\|X_{ia}-X_{jb}\|_1}{t}), & if\ X_{ia}\ and\ X_{jb}\ are\ \text{“}connected\text{”} \\ 0, & else \end{cases} \tag{8}$$

Let $Leighby_{ia}$ and $Leighby_{jb}$ denote the labels of the K-nearest neighbors of X_{ia} and X_{jb}, which are measured by 1-norm distance. If $label_{ia} \in Leighby_{jb}$ and $label_{jb} \in Leighby_{ia}$, X_{ia} would be thought “connected” with X_{jb}. Taking this approach, the category discriminant information is introduced. Then we would put an edge between X_{ia} and X_{jb} based on 1-norm distance as Eq. (8) shows.

Furthermore, for the v views, MvLLS protects all connections between each pair views:

$$\min_{y^1,\cdots,y^v} \sum_{1\le i,j\le v} \xi(i,j) = \sum_{1\le i,j\le v} y^i L^{ij} y^{jT} \tag{9}$$

$$= \begin{bmatrix} y^1, y^2, \cdots, y^v \end{bmatrix} \begin{bmatrix} L^{11} & L^{12} & \cdots & L^{1v} \\ L^{21} & L^{22} & \cdots & L^{2v} \\ \vdots & \vdots & \vdots & \vdots \\ L^{v1} & L^{v2} & \cdots & L^{vv} \end{bmatrix} \begin{bmatrix} y^{1T} \\ y^{2T} \\ \vdots \\ y^{vT} \end{bmatrix}$$

$$= \mathcal{Y}\mathcal{L}\mathcal{Y}^T \tag{10}$$

$$s.t.\ \mathcal{Y}\mathcal{D}\mathcal{Y}^T = 1 \tag{11}$$

where $\mathcal{Y} = [y^1, y^2, \cdots, y^v]$, $\mathcal{L}$ is composed of $[L^{11}, \cdots, L^{vv}]$ as shown above. Moreover, $\mathcal{W}$ is composed of $[W^{11}, \cdots, W^{vv}]$:

$$\mathcal{W} = \begin{bmatrix} W^{11} & W^{12} & \cdots & W^{1v} \\ W^{21} & W^{22} & \cdots & W^{2v} \\ \vdots & \vdots & \vdots & \vdots \\ W^{v1} & W^{v2} & \cdots & W^{vv} \end{bmatrix} \tag{12}$$

$\mathcal{W}$ is the global laplacian weighted graph (GLWP). L^{ij} is not a square matrix always, as n_i may differ from n_j. But when we come to all v views in Eq. (10), $\mathcal{L}$, $\mathcal{W}$ and $\mathcal{D}$ are exactly square matrices. Lagrange multiplier method is then employed to obtain the optimum solution of this problem, and the constraint that $\mathcal{Y}\mathcal{D}\mathcal{Y}^T = 1$ ensures this problem has a unique solution. Finally, this problem boils down to a problem of getting the smallest nonzero generalized eigenvalue and feature vector:

$$\mathcal{L}\mathcal{Y}^T = \lambda\mathcal{D}\mathcal{Y}^T \tag{13}$$

How does GLWP introduce category discriminant information and protect the local structure at the same time? On the one hand, category information determines whether samples are connected or not, such that category discriminant is introduced. And samples of the same class are always connected with each other, as their K-nearest neighbors include themselves. Samples of different classes are still connected, if they are within the K-nearest neighbors of each other. On the other hand, MvLLS expects to find a subspace where the connected samples stay close as well. Therefore, all of the within-class or adjacent samples tend to stay close in the subspace, while between-class samples that are nonadjacent would have no effect to the subspace.

3.3. Laplacian partial least squares

Inspired by PLS, LPLS supposes that embeddings of all samples on each dimension of the subspace have a variation connected with $\mathcal{W}$, and LPLS tries

to make the residual error of $\mathcal{W}$ be small when all variations are removed. After getting $\mathcal{W}$, we can get embeddings of all samples on the first dimension of the subspace $\mathcal{Y}_1$ according to Section 3.2. LPLS uses $\mathcal{Y}_1$ as the regressor of $\mathcal{W}$ to predict $\mathcal{W}$. Then LPLS removes the variation var_1 estimated by $\mathcal{Y}_1$ from $\mathcal{W}$ [43], var_1 is supposed to be as close to $\mathcal{W}$ as possible:

$$\begin{aligned} \mathcal{W} &= var_1 + E_1 \\ var_1 &= P_1^T \mathcal{Y}_1 \end{aligned} \tag{14}$$

where var_1 is the variation predicted by $\mathcal{Y}_1$, E_1 is the residual matrix indicating the residual error that could not be reflected or predicted by $\mathcal{Y}_1$. And $P_1 \in \mathbb{R}^{1\times(n_1+\cdots+n_v)}$ is a loading vector that describes how closely $\mathcal{W}$ is related to $\mathcal{Y}_1$. Then least square method is used to solve this problem, and the variation var_1 is removed from $\mathcal{W}$:

$$\begin{aligned} P_1 &= \frac{\mathcal{Y}_1 \mathcal{W}}{\mathcal{Y}_1 \mathcal{Y}_1^T} \\ E_1 &= \mathcal{W} - var_1 \end{aligned} \tag{15}$$

As shown in Eq. (15), residual matrix E_1 is got by removing the predicted variation var_1 from $\mathcal{W}$. Then we get the new GLWP $\mathcal{W}_2$:

$$\mathcal{W}_2 = (E_1 + E_1^T)/2 \tag{16}$$

After that, the negative values of $\mathcal{W}_2$ is set to zeroes. With the new GLWP $\mathcal{W}_2$, we can get embeddings of all samples on the second dimension of the subspace $\mathcal{Y}_2$ using Eq. (9), $\mathcal{Y}_2$ is used as regressor to predict $\mathcal{Y}_2$ and get var_2 once again. This procedure is repeated for *dim* times to get the embeddings on each dimension of the target subspace, samples of the subspace would reflect the global laplacian weighted graph better.

3.4. Weighted local preserving embedding

As MvLLS is a nonlinear method, it could not get the embeddings of new samples directly. In order to meet the requirements of large-scale applications,

an out-of-sample method weighted local preserving embedding (WLPE) is introduced for MvLLS. Inspired by the work of [44], WLPE finds an embedding in the subspace that maintains the local neighborhood structures of the high-dimensional space. WLPE keeps the global nonlinearity of MvLLS from the local linear fits. Firstly, we get the 1-norm measured K-nearest neighbors for every sample in the original space, which includes samples from all views. Then we characterize the local neighborhood structure by linear confidence, in other words, each sample is represented by a linearly weighted sum of its neighbors across all views. Reconstruction error is minimized in Eq. (17) to get the weights:

$$\begin{aligned} \min_{M} \epsilon(M) \sum_{1\leq a\leq n} \|x_a - \sum_{1\leq b\leq K} M_{ab} x_b\|_F^2 \\ s.t. \sum_b M_{ab} = 1 \end{aligned} \tag{17}$$

In Eq. (17), x_b is one of the K neighbors of x_a, M_{ab} shows the contribution of x_b to the reconstruction of x_a. Lagrangian multiplier method is then employed to get the optimum solution:

$$\begin{aligned} M_a &= \frac{1}{2}\lambda (G_a G_a^T)^{-1} e \\ G_a &= \Big[M_{a1}, M_{a2}, \cdots, M_{ak}\Big] \begin{bmatrix} x_a - x_1 \\ x_a - x_2 \\ \vdots \\ x_a - x_k \end{bmatrix} \end{aligned} \tag{18}$$

In Eq. (18), e is an all ones vector. As $\sum_b M_{ab} = 1$:

$$M_a^T e = 1 \tag{19}$$

Then:

$$1 = e^T M_a = \frac{1}{2}\lambda e^T (G_a G_a^T)^{-1} e \tag{20}$$

with which λ is got. After that, M_a could be got with Eq. (18). The neighbors that weighted greater in $\mathcal{W}$ are expected to be more confident:

$$M'_{ab} = M_{ab} + \sum_{1 \le i \le n_1 + \cdots + n_v} \mathcal{W}_{bi} \tag{21}$$

Then M' is normalized. Afterwords, M' is used to predict the low-dimensional embeddings of new samples. Embedding of the sample a would be represented as Eq. (22) shows:

$$y_a = \sum_{1 \le b \le K} y_b M'_{ab} \tag{22}$$

Finally, the precess of MvLLS is summarized in Algorithm 1.

Algorithm 1 MvLLS

Input: $X_1, \cdots, X_v$, $Label_1, \cdots, Label_v$, dim, K, a new sample x_a.

Output: $Y_1, Y_2 \cdots, Y_v$, embedding of the new sample y_a.

1: Project $X_1, X_2 \cdots, X_v$ and x_a to a common space with a DR framework.
2: Obtain $W^{11}, \cdots, W^{vv}$, piece them into $\mathcal{W}$ and obtain $\mathcal{L}$, $i = 1$.
3: **Repeat**
4: Obtain the embedding of samples on the i^{th} dimension of the subspace $\mathcal{Y}_i$ with Eq. (13);
5: Project $\mathcal{W}$ on $\mathcal{Y}_i$, remove the predicted variation from $\mathcal{W}$ to obtain a new graph with Eq. (15);
6: Make the new graph a symmetric and nonzero matrix;
7: Replace $\mathcal{W}$ with the new graph, construct the new $\mathcal{L}$ and $\mathcal{D}$;
8: **Until** i is equal to dim
9: Obtain embeddings on all dimensions $\mathcal{Y} = [\mathcal{Y}_1; \mathcal{Y}_2; \cdots; \mathcal{Y}_{dim}]$;
10: Obtain the K neighbors y_b and reconstruction contribution matrix M' of x_a with Eq. (18) and Eq. (21);
11: Y_1 is set as the first n_1 columns of $\mathcal{Y}$, Y_2 is set as the second n_2 columns of $\mathcal{Y}$, $\cdots$, Y_v is the last n_v columns of $\mathcal{Y}$;

12: $y_a = \sum_{1 \le b \le K} y_b M'_{ab}$.

13: Output $Y_1, Y_2 \cdots, Y_v$ and y_a.

3.5. Extensions

In this section, we further present some extensions of MvLLS in detail.

(1) The unsupervised and semi-supervised versions of MvLLS. As the construction of $\mathcal{W}$ is very flexible, MvLLS has its unsupervised and semi-supervised versions. We reconstruct W^{ij} with x_{ia} and x_{jb} here, then the new $\mathcal{W}$ can be pieced up. For unsupervised learning, if neither $label_a^i$ nor $label_b^j$ are given, x_{ia} and x_{jb} would be "connected" when $\|x_{ia} - x_{jb}\|_2^2 < \epsilon$, where ϵ is an adjustable parameter. For semi-supervised learning, if $label_a^i$ is given while $label_b^j$ is not, they would be "connected" when both of the two samples are within the K-nearest neighbors of each other, or $label_{ia} \in Leighby_{jb}$. Of course, there could be many other construction method based on different starting points or optimization targets.

(2) Estimation of intrinsic dimension of the subspace. As the global laplacian weighted graph $\mathcal{W}$ upgrades gradually with each iteration, the intrinsic dimension could be estimated when $\mathcal{W}$ tends to be stable. Suppose that the weighted graph after a single iteration is $\mathcal{W}'$, we would think the subspace is stable when $\|\mathcal{W}' - \mathcal{W}\|_F^2 < \epsilon$, where ϵ is an adjustable parameter.

4. Experiments

In this section, we compare the performance of MvLLS with some state-of-art methods on two human emotion datasets: RGB-D human video-emotion dataset and KDEF human face-emotion dataset. We evaluate the proposed method on human emotion recognition of multi-sensor, multi-pose, and multi-feature. Many experiments are designed to show the effeteness and robustness of MvLLS, detailed discussions and comparisons are presented as well.

4.1. Dataset descriptions and feature representations

RGB-D human video-emotion dataset [45] includes 4224 clips of RGB video and 4224 clips of Depth video belonging to 7 emotion categories: angry, disgusted, fearful, happy, neutral, sad, and surprised. To get these clips, professional actors were employed to perform human emotion scripts that are designed under psychological principles. In Fig. 2, some discontinuous frames show a performance of sad emotion, from right, middle and left.

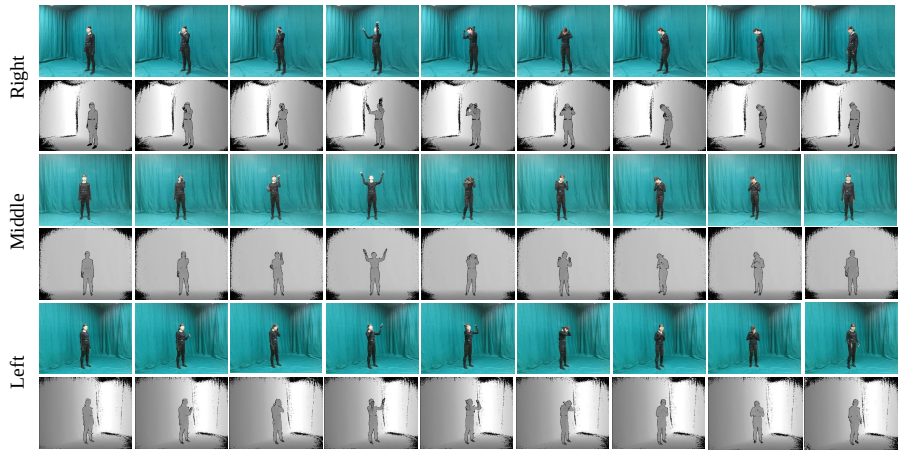

Fig. 2: An example of sad emotion from RGB-D human video-emotion dataset.

For the RGB-D human video-emotion dataset, we extracted the 3-Dimensional Convolutional Neural Networks (3D-CNN) feature, which is a popular and effective method for video learning and feature extraction. As a modified version of BVLC_caffe to support 3D-CNN, C3D-1.0 [46, 47, 48] trained on UCF-101 [49] is used to extract the features. And features of RGB view and Depth view both have a dimension of 4096.

Karolinska Directed Emotional Faces (KDEF) dataset [50, 51] consists of 4900 pictures of 7 human facial emotions: afraid, angry, disgusted, happy, neutral, sad, surprised. A total number of 70 participants were employed to perform these emotions from 5 angles: full left, half left, straight, half right and full right. In this paper we select angles of half left, half right and straight, which include

2940 images totally. Fig. 3 shows examples of surprised, angry and happy emotions from half left, straight and half right angles in KDEF dataset.

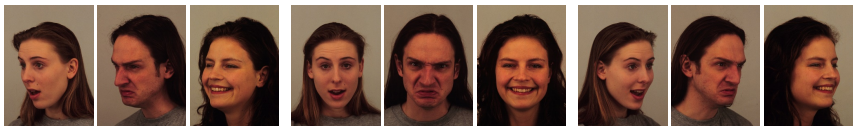

Fig. 3: Examples of surprised, angry and happy from three different angles in KDEF dataset.

For the KDEF dataset, three features are extracted for each selected image with the 2nd last layer of Xception network [52], the 2nd last layer of Inception network [53], and the 6th last layer of MobileNet [54]. All networks are pretrained on ImageNet [55]. Dimensions of the features are 2048, 1024 and 2048 respectively.

4.2. Comparison methods and experimental setting

We evaluate the proposed method with as many as two-view and multi-view learning methods that we can compare with, including CCA, PLS, MCCA, MULDA, GMA, MvDA and MvDA-VC. All experiments about the comparison methods are conducted with available codes.

After extracting the features of both datasets, C3D feature of RGB view and Depth view from the RGB-D human video-emotion dataset are used in human emotion recognition across sensors (multi-sensor task); MobileNet feature of half left, half right and straight angles of KDEF dataset are used in human emotion recognition across poses (multi-pose task); and Xception feature, Inception feature, and MobileNet feature of straight view in KDEF dataset are used in human emotion recognition across features (multi-feature task).

Averaged classification accuracy is used to evaluate the performance of different methods. Each experiment is randomly repeated for 10 times and the results are averaged. If there is no special explanation, the dimension of subspace *dim* of each experiment is set to the minimum of its all views, to preserve as much as energy. DR framework used in the experiments is PCA [42], as

PCA may be the most classical, effective and widely used DR framework. In multi-sensor experiments, the parameter t of Eq. (8) is set to 1000, the number of neighbors K is set to 50; in multi-pose and multi-feature experiments, t is set to 200 and K is set to 300. And extreme learning machine (ELM) [56] is used as the classifier for all experiments. ELM is a classical feedforward network with a single hidden layer, the number of hidden layer node is set to 8000, with *sigmoid* function as the activation function.

4.3. Comparisons and evaluations

4.3.1. Evaluation as a whole

In this section, we compare MvLLS with some two-view or multi-view learning method on the three tasks, 2/3 data of each view is randomly selected for training with the others for testing. Table 2 and Table 3 show the average accuracy of each view for both datasets before the subspace learning. Table 4 shows the comparisons between MvLLS and many other methods on human emotion recognition of the multi-sensor, multi-pose and multi-feature task. CCA and PLS could not be used in multi-pose task and multi-feature task as they are two-view learning methods, such that the corresponding spaces in Table 4 are marked as "-". Experimental results indicate that MvLLS performs better than other methods. In the multi-sensor emotion recognition task, average classification accuracy is improved by 2.42% (=48.41%-45.59%) from MvDA-VC, the best performing comparison method. And in the multi-pose emotion recognition task, the average accuracy is improved by 4.38% (=74.02%-69.64%) from MvDA-VC; in the multi-feature emotion recognition task, the average accuracy is improved by 3.57% (75.71%-72.14%) from MvDA-VC. Specially, it can be observed that MvLLS performs better than any single view before multi-view learning.

The improvements of MvLLS in average accuracy could be boiled down to its great nonlinear learning, scatter discriminant balance and locality protection characters. CCA and GMA perform poorly as the inter-view and intra-view information is not considered. By using iterative approximation, PLS performs

Table 2: The average accuracy of each view for RGB-D video-emotion dataset (%)

Feature	RGB view	Depth view
C3D feature	37.97	31.72

Table 3: The average recognize accuracy of each view for KDEF dataset (%)

Feature	Half Left	Half Right	Straight
Xception feature	64.11	65.09	72.18
Inception feature	56.50	57.79	68.07
MobileNet feature	66.27	66.07	73.74

Table 4: Comparisons on three tasks in terms of average accuracy (%)

Task	CCA	PLS	MCCA	MULDA	GMA	MvDA	MvDA-VC	MvLLS
Multi-sensor	13.08	40.63	15.15	32.63	35.20	43.65	45.99	48.41
Multi-pose	-	-	35.02	43.21	47.50	61.07	69.64	74.02
Multi-feature	-	-	38.57	46.63	56.79	60.02	72.14	75.71

much better than CCA. MvDA jointly learns between-class variation and within-class variation across all views, while the entirety of each view and locality is not taken into consideration. And MvDA-VC has a significant improvement than MvDA by adding view-consistency. The proposed method MvLLS takes advantages of PLS, category discriminant information and locality information, then get better performance in average accuracy.

4.3.2. Evaluation with different training sizes

To analyze the robustness of the proposed method, we evaluate the average classification accuracy with different training sizes. Multi-pose and multi-feature task are taken as examples. Fig. 4 and Fig. 5 show the accuracies with different training sizes for multi-pose and multi-feature task respectively. The training size is setted in change interval of [10, 90] (%) with the step size of 10. And from these tables, we can observe that MvLLS outperforms than all related methods with different training size.

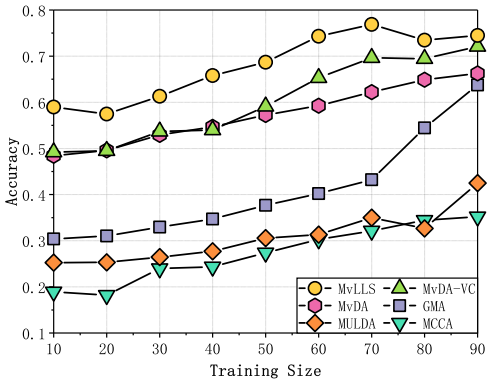

Fig. 4: Comparisons of average accuracy for multi-pose task with different training Sizes.

When training size is extremely low, all methods could not learn enough information. When training size is high enough, MvDA, MvDA-VC and MvLLS learn surplus information. When the training size is close to 50%, MvLLS performs much better than other methods. That is because MvLLS could make full use of category discriminant information and local neighborhood information,

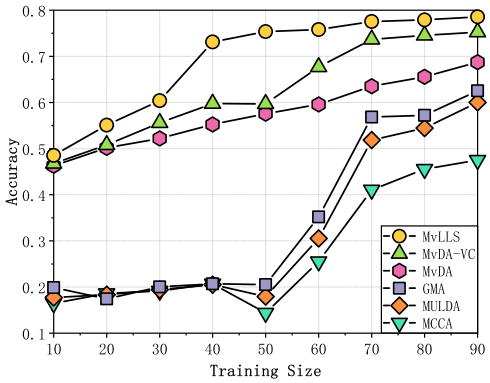

Fig. 5: Comparisons of average accuracy for multi-feature task with different training sizes.

and WLPE gets new samples involved in known samples very well. MvDA and MvDA-VC focus more on scatter discriminant information, GMA just consider the cross correlations, MULDA ignores the local structure as well.

4.3.3. Evaluation with different dimensions of the subspace

In this section we compare the performance of each method on different dimensions of the subspace. Multi-pose task and multi-feature task are taken as examples as well. For the both tasks, *dim* varies in change interval of [100, 1000] with the step size of 100. Fig. 6 and Fig. 7 indicate that MvLLS could get the best classification accuracy as *dim* varies.

MvLLS performs well when *dim* is extremely low, which means the subspace got by MvLLS is more representative and typical. Furthermore, MvLLS performs better and better as *dim* improves, because MvLLS is a nonlinear method optimized with iteration method. MvLLS removes the estimated variations of the embeddings gradually to get a proper solution, while other methods get linear transformers directly.

4.3.4. Evaluation of the effectiveness of interactive method

To analyse the effectiveness of interactive method used in MvLLS, we conduct experiments on the three tasks to compare the average accuracy between

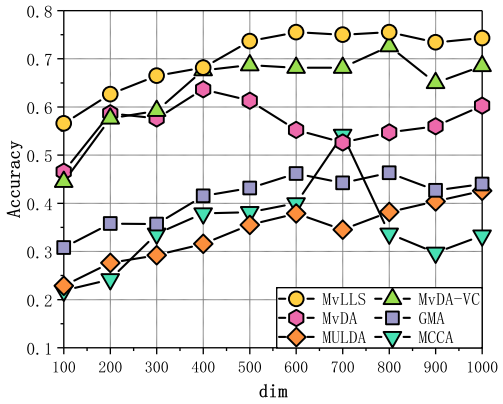

Fig. 6: Comparisons of average accuracy for multi-pose task on different target dimensions.

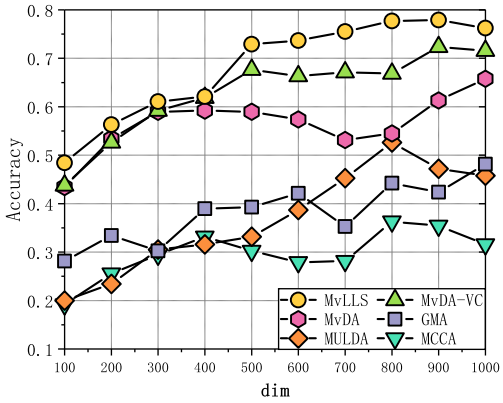

Fig. 7: Comparisons of average accuracy for multi-feature task on different target dimensions.

MvLLS and its non-iterative version (called $\text{MvLLS}_{\text{noITE}}$). Similarly, 2/3 data of each view is used as the training set with the others as the test set. From Table 8 it can be observed that the average classify accuracy is improved by nearly 1% for each task when iterative method is used.

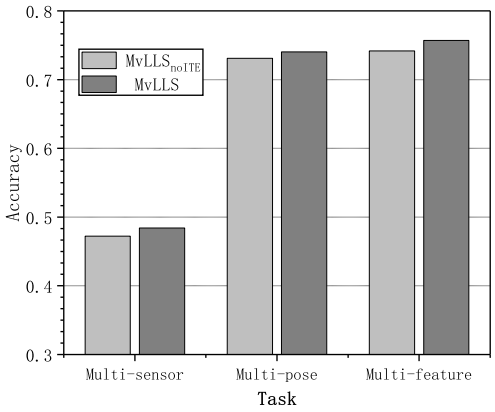

Fig. 8: Comparisons of average accuracy between MvLLS and $\text{MvLLS}_{\text{noITE}}$

4.3.5. Evaluation of influence of the parameters

The coefficient t and the number of neighbor K in the neighborhood are two important parameters in MvLLS. Taking the multi-sensor task as an example, we conduct experiments to evaluate the influence of the two parameters. In Table 5, K is set as 50 and t varies in the interval of [600, 1400] with the step size of 100. And in Table 6, t is set as 1000 and K varies in the interval of [10, 90] with the step size of 10. We can draw the conclusion that t has little influence on MvLLS, but MvLLS performs worse when the value of K is extremely low. That is due to each sample would not be represented well and not many samples would be connected. In general, MvLLS has fine robustness as parameter varies.

Table 5: Influence of t in the multi-sensor recognition task (%)

t	600	700	800	900	1000	1100	1200	1300	1400
Accuracy	48.33	48.41	48.72	48.25	48.88	48.64	48.52	48.71	48.53

Table 6: Influence of K in the multi-sensor recognition task (%)

K	10	20	30	40	50	60	70	80	90
Accuracy	43.86	46.53	47.17	48.28	48.41	48.33	48.41	48.64	48.32

4.3.6. Time consuming evaluation

This section reports the average consuming time of MvLLS and related methods on the three tasks, Table 7 lists the training time and testing time of the methods on each task. The computer configuration we used in this experiment is i3-2120(3.30GHz), 16 GB memory with 64-bit computer system. As the price of better performance and robustness, MvLLS takes more time than other methods, because the construction of GLWP and iterative process are really time-consuming. MvLLS needs to construct a global graph GLWP to explore local structure and category discriminant information. Iterative method is used to make the proposed method more robust, and make distributions of samples in the subspace fit the global graph better. As for the test data, MvLLS also needs to take some time to get the local reconstruction weights to keep the nonlinearity.

Table 7: Average time consuming of MvLLS and related methods on three tasks (s)

Method	Multi-sensor		Multi-pose		Multi-feature	
	Training	Testing	Training	Testing	Training	Testing
CCA	52.52	1.02	-	-	-	-
PLS	128.32	1.05	-	-	-	-
MCCA	11.03	0.21	2.28	0.14	15.76	0.95
MULDA	63.41	0.84	58.93	0.42	136.47	0.84
GMA	570.16	0.79	20.02	0.03	60.59	0.06
MvDA	10.48	1.16	3.97	0.65	14.50	0.80
MvDA-VC	10.94	0.71	2.85	0.50	15.18	0.78
MvLLS	2184.21	57.88	495.03	7.90	984.38	14.43

5. Conclusion

In this paper, a flexible and extensible nonlinear method multi-view laplacian least square (MvLLS) is proposed for multi-view human-emotion recognition. MvLLS finds a common subspace across all views where the connected samples stay close to each other as well. With the global laplacian weighted graph (GLWP), MvLLS introduces the category discriminant information and protects the local neighborhood information. MvLLS is optimized with interactive method, and the weighted local preserving embedding (WLPE) is the out-of-sample extension of MvLLS. Experimental results verified the effectiveness and robustness of the proposed method.

The main drawback of the proposed method is the high time complexity. In the future, we will work to reduce the time complexity of MvLLS, and evaluate MvLLS with more datasets.

Acknowledgements

This study was funded by National Natural Science Foundation of People's Republic of China (No. 61672130, 61602082, 91648205), the National Key Scientific Instrument and Equipment Development Project (No. 61627808), the Development of Science and Technology of Guangdong Province Special Fund Project Grants (No. 2016B090910001). the LiaoNing Revitalization Talents Program (MO. XLYC1806006). All the authors declare that they have no conflict of interest.

References

[1] H. Rosenberg, S. McDonald, M. Dethier, R. P. Kessels, R. F. Westbrook, Facial emotion recognition deficits following moderate–severe traumatic brain injury (tbi): Re-examining the valence effect and the role of emotion intensity, Journal of the International Neuropsychological Society 20 (10) (2014) 994–1003.

[2] S. Ebrahimi Kahou, V. Michalski, K. Konda, R. Memisevic, C. Pal, Recurrent neural networks for emotion recognition in video, in: Proceedings of the 2015 ACM on International Conference on Multimodal Interaction, ACM, 2015, pp. 467–474.

[3] Y. Fan, X. Lu, D. Li, Y. Liu, Video-based emotion recognition using cnn-rnn and c3d hybrid networks, in: Proceedings of the 18th ACM International Conference on Multimodal Interaction, ACM, 2016, pp. 445–450.

[4] B. Schuller, G. Rigoll, M. Lang, Hidden markov model-based speech emotion recognition, in: Acoustics, Speech, and Signal Processing, 2003. Proceedings.(ICASSP'03). 2003 IEEE International Conference on, Vol. 2, IEEE, 2003, pp. II–1.

[5] A. M. Bhatti, M. Majid, S. M. Anwar, B. Khan, Human emotion recognition and analysis in response to audio music using brain signals, Computers in Human Behavior 65 (2016) 267–275.

[6] X. Huang, W. Wu, H. Qiao, Y. Ji, Brain-inspired motion learning in recurrent neural network with emotion modulation, IEEE Transactions on Cognitive and Developmental Systems 10 (4) (2018) 1153–1164.

[7] P. Yin, H. Qiao, W. Wu, L. Qi, Y. Li, S. Zhong, B. Zhang, A novel biologically inspired visual cognition model: Automatic extraction of semantics, formation of integrated concepts, and reselection features for ambiguity, IEEE Transactions on Cognitive and Developmental Systems 10 (2) (2018) 420–431.

[8] S. E. Kahou, C. Pal, X. Bouthillier, P. Froumenty, Ç. Gülçehre, R. Memisevic, P. Vincent, A. Courville, Y. Bengio, R. C. Ferrari, et al., Combining modality specific deep neural networks for emotion recognition in video, in: Proceedings of the 15th ACM on International conference on multimodal interaction, ACM, 2013, pp. 543–550.

[9] Z. Tong, W. Zheng, C. Zhen, Z. Yuan, J. Yan, K. Yan, A deep neural network driven feature learning method for multi-view facial expression recognition, IEEE Transactions on Multimedia 18 (12) (2016) 2528–2536.

[10] Z. Zhang, F. Ringeval, B. Dong, E. Coutinho, E. Marchi, B. Schuller, Enhanced semi-supervised learning for multimodal emotion recognition, in: IEEE International Conference on Acoustics, 2016.

[11] C. Xu, D. Tao, C. Xu, A survey on multi-view learning, arXiv preprint arXiv:1304.5634.

[12] C. Zhang, H. Fu, Q. Hu, X. Cao, Y. Xie, D. Tao, D. Xu, Generalized latent multi-view subspace clustering, IEEE transactions on pattern analysis and machine intelligence.

[13] H. Hotelling, Relations between two sets of variates, Biometrika 28 (3/4) (1936) 321–377.

[14] M. Belkin, P. Niyogi, Laplacian eigenmaps for dimensionality reduction and data representation, Neural computation 15 (6) (2003) 1373–1396.

[15] S. Akaho, A kernel method for canonical correlation analysis, arXiv preprint cs/0609071.

[16] J. Rupnik, J. Shawe-Taylor, Multi-view canonical correlation analysis, in: Conference on Data Mining and Data Warehouses (SiKDD 2010), 2010, pp. 1–4.

[17] A. Sharma, D. W. Jacobs, Bypassing synthesis: Pls for face recognition with pose, low-resolution and sketch.

[18] R. Rosipal, L. J. Trejo, Kernel partial least squares regression in reproducing kernel hilbert space, Journal of machine learning research 2 (Dec) (2001) 97–123.

[19] J. Farquhar, D. Hardoon, H. Meng, J. S. Shawe-taylor, S. Szedmak, Two view learning: Svm-2k, theory and practice, in: Advances in neural information processing systems, 2006, pp. 355–362.

[20] S. Szedmak, J. Shawe-Taylor, Synthesis of maximum margin and multiview learning using unlabeled data, Neurocomputing 70 (7-9) (2007) 1254–1264.

[21] H. Liu, L. Liu, T. D. Le, I. Lee, S. Sun, J. Li, Nonparametric sparse matrix decomposition for cross-view dimensionality reduction, IEEE Transactions on Multimedia 19 (8) (2017) 1848–1859.

[22] J. Li, H. Yong, B. Zhang, M. Li, L. Zhang, D. Zhang, A probabilistic hierarchical model for multi-view and multi-feature classification, in: Thirty-Second AAAI Conference on Artificial Intelligence, 2018.

[23] R. O. Duda, P. E. Hart, Pattern classification and scene analysis, A Wiley-Interscience Publication, New York: Wiley, 1973.

[24] Y. Ma, S. Lao, E. Takikawa, M. Kawade, Discriminant analysis in correlation similarity measure space, in: Proceedings of the 24th international conference on Machine learning, ACM, 2007, pp. 577–584.

[25] A. Sharma, A. Kumar, H. Daume, D. W. Jacobs, Generalized multiview analysis: A discriminative latent space, in: Computer Vision and Pattern Recognition (CVPR), 2012 IEEE Conference on, IEEE, 2012, pp. 2160–2167.

[26] M. Kan, S. Shan, H. Zhang, S. Lao, X. Chen, Multi-view discriminant analysis, IEEE transactions on pattern analysis and machine intelligence 38 (1) (2016) 188–194.

[27] S. Sun, X. Xie, M. Yang, Multiview uncorrelated discriminant analysis, IEEE transactions on cybernetics 46 (12) (2016) 3272–3284.

[28] Z. Jin, J. Y. Yang, Z. S. Hu, Z. Lou, Face recognition based on the uncorrelated discriminant transformation, Pattern Recognition 34 (7) (2001) 1405–1416.

[29] G. Cao, A. Iosifidis, K. Chen, M. Gabbouj, Generalized multi-view embedding for visual recognition and cross-modal retrieval, IEEE transactions on cybernetics 48 (9) (2018) 2542–2555.

[30] Y. H. Yuan, Y. Li, X. B. Shen, Q. S. Sun, J. L. Yang, Laplacian multiset canonical correlations for multiview feature extraction and image recognition, Multimedia Tools & Applications 76 (1) (2017) 731–755.

[31] L. Han, X.-Y. Jing, F. Wu, Multi-view local discrimination and canonical correlation analysis for image classification, Neurocomputing 275 (2018) 1087–1098.

[32] J. Yu, C. Zhu, J. Zhang, Q. Huang, D. Tao, Spatial pyramid-enhanced netvlad with weighted triplet loss for place recognition, IEEE Transactions on Neural Networks and Learning Systems.

[33] T. Xia, D. Tao, T. Mei, Y. Zhang, Multiview spectral embedding, IEEE Transactions on Systems, Man, and Cybernetics, Part B (Cybernetics) 40 (6) (2010) 1438–1446.

[34] Wang, Fengshan, Zhang, Daoqiang, A new locality-preserving canonical correlation analysis algorithm for;multi-view dimensionality reduction, Neural Processing Letters 37 (2) (2013) 135–146.

[35] J. Wu, Z. Lin, W. Zheng, H. Zha, Locality-constrained linear coding based bi-layer model for multi-view facial expression recognition, Neurocomputing 239 (C) (2017) 143–152.

[36] Y. H. Yuan, Q. S. Sun, Graph regularized multiset canonical correlations with applications to joint feature extraction, Pattern Recognition 47 (12) (2014) 3907–3919.

[37] W. Liu, X. Yang, D. Tao, J. Cheng, Y. Tang, Multiview dimension reduction via hessian multiset canonical correlations, Information Fusion 41 (2017) S1566253517300519.

[38] J. Yu, C. Hong, Y. Rui, D. Tao, Multi-task autoencoder model for recovering human poses, IEEE Transactions on Industrial Electronics 65 (6) (2018) 5060–5068.

[39] J. Wang, Z. Rui, W. Yang, C. Zheng, J. Kong, Y. Yi, Locality constrained graph optimization for dimensionality reduction, Neurocomputing 245 (2017) 55–67.

[40] Z. Zhichao, S. Huaijiang, Z. Guoqing, Multiple kernel locality-constrained collaborative representation-based discriminant projection for face recognition, Neurocomputing.

[41] C. Hong, J. Yu, D. Tao, W. Meng, Image-based three-dimensional human pose recovery by multiview locality-sensitive sparse retrieval, IEEE Transactions on Industrial Electronics 62 (6) (2015) 3742–3751.

[42] I. Jolliffe, Principal component analysis, in: International encyclopedia of statistical science, Springer, 2011, pp. 1094–1096.

[43] J. Trygg, S. Wold, Orthogonal projections to latent structures (o-pls), Journal of Chemometrics: A Journal of the Chemometrics Society 16 (3) (2002) 119–128.

[44] L. K. Saul, S. T. Roweis, Think globally, fit locally: unsupervised learning of low dimensional manifolds, Journal of machine learning research 4 (Jun) (2003) 119–155.

[45] S. Liu, S. Guo, H. Qiao, Y. Wang, B. Wang, W. Luo, M. Zhang, K. Zhang, B. Du, Multi-view Laplacian Eigenmaps Based on Bag-of-Neighbors For RGBD Human Emotion Recognition, arXiv e-prints`arXiv:1811.03478`.

[46] D. Tran, L. Bourdev, R. Fergus, L. Torresani, M. Paluri, Learning spatiotemporal features with 3d convolutional networks, in: Proceedings of the IEEE international conference on computer vision, 2015, pp. 4489–4497.

[47] Y. Jia, E. Shelhamer, J. Donahue, S. Karayev, J. Long, R. Girshick, S. Guadarrama, T. Darrell, Caffe: Convolutional architecture for fast feature embedding, in: Proceedings of the 22nd ACM international conference on Multimedia, ACM, 2014, pp. 675–678.

[48] A. Karpathy, G. Toderici, S. Shetty, T. Leung, R. Sukthankar, L. Fei-Fei, Large-scale video classification with convolutional neural networks, in: Proceedings of the IEEE conference on Computer Vision and Pattern Recognition, 2014, pp. 1725–1732.

[49] K. Soomro, A. R. Zamir, M. Shah, Ucf101: A dataset of 101 human actions classes from videos in the wild, arXiv preprint arXiv:1212.0402.

[50] D. Lundqvist, A. Flykt, A. Öhman, The karolinska directed emotional faces (kdef), CD ROM from Department of Clinical Neuroscience, Psychology section, Karolinska Institutet 91 (1998) 630.

[51] D. Lundqvist, J. Litton, The averaged karolinska directed emotional faces, Stockholm: Karolinska Institute, Department of Clinical Neuroscience, Section Psychology.

[52] F. Chollet, Xception: Deep learning with depthwise separable convolutions, in: Proceedings of the IEEE conference on computer vision and pattern recognition, 2017, pp. 1251–1258.

[53] C. Szegedy, V. Vanhoucke, S. Ioffe, J. Shlens, Z. Wojna, Rethinking the inception architecture for computer vision, in: Proceedings of the IEEE conference on computer vision and pattern recognition, 2016, pp. 2818–2826.

[54] A. G. Howard, M. Zhu, B. Chen, D. Kalenichenko, W. Wang, T. Weyand, M. Andreetto, H. Adam, Mobilenets: Efficient convolutional neural networks for mobile vision applications, arXiv preprint arXiv:1704.04861.

[55] J. Deng, W. Dong, R. Socher, L.-J. Li, K. Li, L. Fei-Fei, Imagenet: A large-scale hierarchical image database, in: 2009 IEEE conference on computer vision and pattern recognition, Ieee, 2009, pp. 248–255.

[56] G.-B. Huang, Q.-Y. Zhu, C.-K. Siew, Extreme learning machine: theory and applications, Neurocomputing 70 (1-3) (2006) 489–501.